Shahid Chamran University of Ahvaz

Irrigation Sciences and Engineering (JISE)
Vol. 47, No. 4, Winter 2025, p. 93-104

Journal homepage: https://jise.scu.ac.ir

Original Paper

Improving Water Diversion Efficiency in Converging Side Weirs through Side Vane Installation: a numerical simulation

Kosar Neysi[1], Mehdi Daryaee[2*], Seyed Mahmood Kashefipour[3], Amirreza Shahriari[4] and Mohammadreza Zayeri[5]

1- *Master Student, Department of Water Structures, Faculty of Water and Environmental Engineering, Shahid Chamran University of Ahvaz, Ahvaz, Iran.*
2*- *Corresponding Author, Associate professor, Department of Water Structures, Faculty of Water and Environmental Engineering, Shahid Chamran University of Ahvaz, Ahvaz, Iran. (M.Daryaee@scu.ac.ir)*
3- *Professor, Department of Water Structures, Faculty of Water and Environmental Engineering, Shahid Chamran University of Ahvaz, Ahvaz, Iran.*
4- *Ph.D Student, Department of Water Structures, Faculty of Water and Environmental Engineering, Shahid Chamran University of Ahvaz, Ahvaz, Iran.*
5- *Assistant professor, Department of Water Structures, Faculty of Water and Environmental Engineering, Shahid Chamran University of Ahvaz, Ahvaz, Iran.*

ARTICLE INFO

Artlcle history:
Received: 24 November 2024
Revised: 3 February 2025
Accepted: 5 February 2025

Keywords:
Converging Side Weir , Flow-3D model , Side vane , hydraulic structure.

TO CITE THIS ARTICLE:

Neysi, K., Daryaee, M., Kashefipour, S. M., Shahriari, A., Zayeri, M. (2025). 'Improving Water Diversion Efficiency in Converging Side Weirs through Side Vane Installation: a numerical simulation', *Irrigation Sciences and Engineering*, 47(4), pp. 93-104. doi: 10.22055/jise.2025.48446.2145.

Abstract

Side weirs are important components in irrigation and drainage systems, used for controlling and diverting flow. Given the advantages of side weirs in converging channels, improving the hydraulic performance of these structures is essential. This study aims to enhance the hydraulic performance of converging side weirs through the installation of a side vane. Numerical simulations were conducted using the Flow-3D software with various turbulence models, and the results were validated against experimental data ($MAPE = 1.62$). In this study, three different angles for side vane installation (60, 90, and 120 degrees) at two positions, upstream and downstream of the weir, were investigated. The results showed that installing the side vane at the upstream position of the weir with a 60-degree angle led to a 32% increase in the diversion flow compared to the control scenario (without side vane). The analysis revealed that the reduction in flow velocity downstream of the side weir and the creation of a low-velocity zone around the side vane contributed to more effective flow guidance toward the weir, thereby increasing its efficiency. The practical application of the results of this research is the improvement of converging side weir design and their enhanced efficiency in managing water flows.

Introduction

Protective structures in irrigation and drainage networks hold significant importance. These structures are designed to safeguard channels and adjacent facilities, preventing damage caused by uncontrolled water inflow into the channels. Side weirs can be considered as protective free-flow structures installed on the sidewalls of the main channel, parallel to its alignment. The hydraulics of these weirs function such that when the water level reaches the crest elevation, the excess flow is discharged through the weir.

Numerous experimental studies have been conducted on side weirs, with most research focusing on enhancing the discharge coefficient of these structures. Emiroglu et al.

(2010), through experimental studies on side weirs in a straight channel, concluded that labyrinth side weirs have a higher discharge coefficient compared to simple rectangular weirs. Vatankhah (2013), following extensive experiments, proposed an analytical solution for determining the water surface profile along a side weir located in a parabolic channel. Karimi et al. (2018), by comparing piano key and rectangular side weirs, found that piano key side weirs exhibit higher discharge coefficients. Parsi et al. (2021), through experimental investigations of the positioning of side weirs on inclined and straight walls, presented a novel relationship based on the critical depth of flow over the weir to determine the diversion flow rate in rectangular channels with downstream contractions. The results showed that the discharge rate of side weirs located on inclined walls is approximately 7.5% higher than that of weirs positioned on straight walls.

Kartal and Emiroglu (2022) conducted experimental studies to examine the subcritical flow characteristics of combined gate-side weirs and proposed equations for calculating the discharge of such systems.

Mirzaei and Sheibani (2021) investigated the hydraulic behavior of sharp-crested arc weirs and compared them with rectangular weirs. They concluded that the discharge coefficient of arc weirs depends on their arc length, with arc weirs demonstrating higher discharge rates compared to rectangular weirs. Ghanbari and Heidarnejad (2020) carried out experiments on piano key side weirs with triangular and rectangular geometries, concluding that the discharge coefficient of triangular piano key weirs is 25% higher than that of rectangular piano key weirs.

Numerical modeling is cost-effective, time-efficient, and enables detailed analysis of complex flow conditions. It allows for parameter adjustments, offering flexibility and precision in improving hydraulic structures. The findings of various researchers indicate that the Flow-3D numerical model performs effectively in simulating side weirs (Saffar et al., 2023; Kalateh and Aminvash, 2023; Bagheri Seyyed Shekari et al., 2018; Parsaie et al., 2022).

Shahriari et al. (2024) utilized Flow-3D simulations to investigate the impact of installing guide vanes (G.V.) on the hydraulic performance of side weirs in converging channels. Their findings revealed that a G.V. enhanced outflow efficiency by 14%, while longer vanes caused a reduction in efficiency due to the formation of vortices.

Ghazizadeh and Moghaddam (2016) investigated side weirs with circular crests using numerical simulations in the Flow-3D software. In their study, they evaluated the effects of upstream and downstream slope variations as well as crest height on pressure distribution and energy dissipation. The results indicated that increasing the upstream slope leads to an approximately 62% increase in the relative flow depth over the crest.

Mohamadalipourahari et al. (2021) analyzed the velocity distribution in rectangular side weirs using Flow-3D software. Their findings included equations for kinetic energy and momentum correction coefficients, as well as the identification of flow separation zones.

Khassaf et al. (2016) modeled compound side weirs in Flow-3D and estimated the discharge coefficient for two types of compound side weirs: rectangular and semi-circular.

Noroozi et al. (2021) investigated compound weirs comprising labyrinth and piano key weirs with vertical walls at the inlet and outlet using numerical simulations. They also presented the discharge coefficient curve for these compound weirs.

The use of side weirs in converging channels, as shown in Figure (1), has garnered attention in research due to their dual functionality as both a converter and a weir (Honar and Javan, 2008; Zarei et al., 2020; Ghorbannia and Eghbalzadeh, 2018). The findings of Maranzoni et al. (2017) indicate that this type of side weir installation leads to increased discharge capacity and water level over the crest.

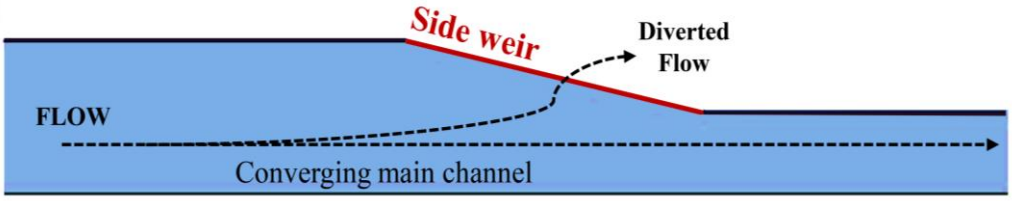

Fig. 1- View of the converging side weir

Saffar et al. (2023) simulated flow in converging side weirs using Flow-3D software and compared the results with experimental data. They found that this numerical model could predict hydraulic parameters with high accuracy. Moreover, they observed that reducing the downstream width increases flow depth and energy upstream, which, even under low discharge conditions, results in flow deviation away from the side weir.

Increasing the outflow discharge to side weirs is one of the key challenges in designing and operating these hydraulic structures. This issue becomes even more critical under conditions of climate change and increased rainfall intensity, which can introduce sudden and unexpected flows into channels. In this study, an innovative approach is proposed to enhance the performance of side weirs by combining two geometric strategies. First, designing the channel as converging, which alters the flow pattern and enhances transverse velocity. Second, installing a side vane on the wall opposite the weir, which is hypothesized to guide flow lines adjacent to the wall toward the weir, thereby increasing the side weir's discharge capacity.

Materials and Metods

Flow-3D is an advanced software in the field of computational fluid dynamics (CFD) capable of simulating a wide range of flows. It describes flow movement by solving the Reynolds-Averaged Navier-Stokes (RANS) equations. Since numerous studies have already elaborated on these equations, this research refrains from further explanation and instead references previous investigations (Taghavi and ghodosi, 2016; Azimi and Shabanlou, 2015; Abbasi et al., 2020; Afaridegan et al., 2023; Parsaie et al., 2018). In this study, the numerical model was calibrated based on the results obtained by Maranzoni et al. (2017), and an appropriate turbulence model was selected for simulating flow in converging side weirs. This process involved comparing experimental data with numerical simulations using reliable statistical indices such as *MAPE*, R^2, and percentage error *(%E*) to assess accuracy (Equation 1).

$$\%E = \frac{\sum_{i=1}^{n} \left|(x_{i_p} - x_{i_m}\right|}{\sum_{i=1}^{n} x_{i_p}} \times 100 \qquad (1a)$$

$$MAPE = \frac{\sum_{i=1}^{n} \left|\frac{(x_{i_p} - x_{i_m}}{x_{i_p}}\right|}{N_t} \times 100 \qquad (1b)$$

In the above equations, x_{i_p} represents the measured experimental values, x_{i_m} refers to the values calculated by the Flow-3D numerical model, and N_t denotes the number of data points. Maranzoni et al. (2017) conducted their experiments in an 11-meter-long experimental flume. The converging section of the channel, where the side weir was located, reduced the channel width from 36 cm (B_1) to 18 cm (B_2) over a distance from 5.45 m to 6.95 m along the flume. The rectangular side weir, with a thickness of 5.5 cm and a length of 1.511 m (L), was positioned within this converging section. The weir had a convergence angle (α) of 7 degrees and a crest height (w) of 18.3 cm. To enhance the diversion flow rate of the weir, a side vane

was installed on the wall opposite the side weir (Figure 2). The length of this vane was set to 20% of the upstream channel width, and its thickness was chosen to be 1.5 cm. The scenarios investigated in this study included installing the side vane at angles of $\theta = 60, 90, 120$ and in two positions, X_1 and X_2. Position X_1 corresponds to the upstream end of the weir, while X_2 corresponds to the downstream start of the weir (Figure 2). The vane height was designed to ensure that the flow conditions around it remained unsubmerged.

In total, 7 simulations were conducted, including the reference simulation. All simulations were carried out at an inlet flow rate of 45 liters per second. In each simulation, the efficiency of the side weir was calculated using Equation 2. In this equation, Q_1 represents the inlet flow rate to the main channel, and Q_d represents the diversion flow rate from the side weir.

$$\varepsilon = \frac{Q_d}{Q_1} \quad (2)$$

Table (1) presents the specifications of the variables for these simulations, including the positioning and installation angle of the side vane.

To complete the simulation process, three mesh blocks were defined for the upstream, weir region, and downstream areas (Figure 3). The mesh sizes for the upstream and downstream blocks were set to 0.016 meters, while for the weir region, the mesh size was reduced to 0.008 meters to ensure greater computational accuracy. In simulations involving the side vane, a separate mesh block with a size of 0.006 meters was assigned to the geometric region of the side vane to accurately capture its geometry. The inlet and outlet boundary conditions are shown in Figure (3). For the boundaries parallel to the walls and bed, the boundary condition "Wall" was applied, and for all other boundaries, the "Symmetry" condition was used.

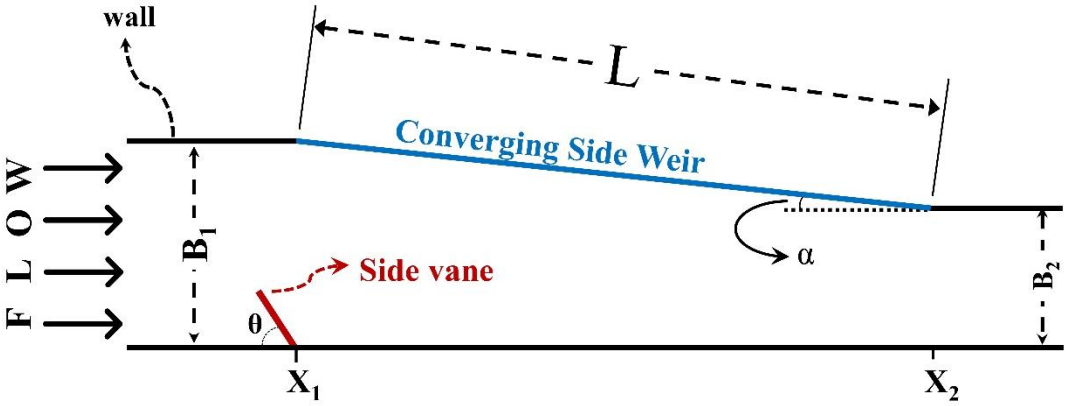

Fig. 2- Top view of the converging side weir showing the geometric parameters and the side vane.

Table 1- Introduction and nomenclature of the simulations in the present study

scenario	position of S.V.	θ (Degree)
Control	-	-
T1	X_1	120
T2		90
T3		60
T4	X_2	120
T5		90
T6		60

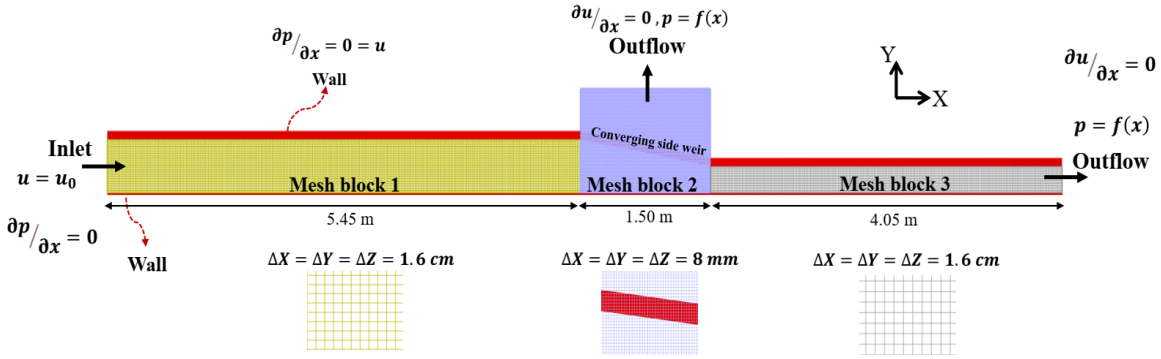

Fig. 3- View of the mesh grid and simulation details

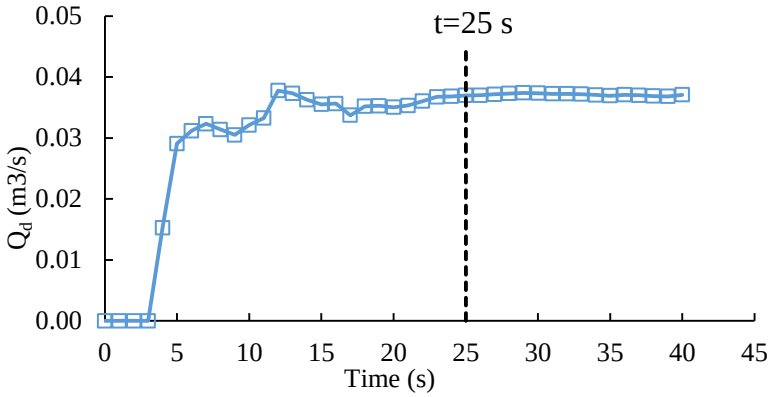

Fig. 4- Time Series of Diversion Flow Rate

Table 2- Comparison of Experimental and Numerical Data

Turbulence Model	E%	MAPE
K − ε	8.71	4.4
K − ω	10.77	5.39
RNG	3.67	1.62

Results and Discussion

In this study, the simulation time was set to 25 seconds, after which the outputs reached a steady state, as shown in Figure (4). The relatively short simulation time, considered an advantage, was due to the creation of a fluid region in the main channel at the crest elevation of the side weir. This approach optimized the simulation process without affecting the flow hydraulics.

Subsequently, the dimensionless ratio of longitudinal velocity to depth-averaged velocity (u/U) was extracted at the mid-section of the side weir and compared with the experimental data of Maranzoni et al. (2017). The mid-section, located exactly at the center of the converging side weir, corresponds to a longitudinal position of $X = 0.75\ m$ from the weir's starting point. Data were collected at two elevation levels near the water surface and one elevation level close to the bed at this section, in accordance with the experimental setup of Maranzoni et al. (2017). The results of this comparison are presented in Table (2). This analysis was performed for different turbulence models in the Flow-3D software. Moreover, σ_ε, σ_K, $C_{1\varepsilon}$, and $C_{2\varepsilon}$ are constants set to 0.7194, 0.7194, 1.68, and 1.42, respectively, in turbulence models. ultimately, the RNG turbulence model was selected as the optimal model for conducting further simulations.

The R^2 value, a key criterion for assessing the fit of the regression model to the data, was calculated after applying the linear regression model to the data obtained from the software and comparing it with the experimental data (Figure 5). In this model, the R^2 value was found to be 0.92, indicating the high efficiency and accuracy of the numerical model in simulating the flow behavior in the side weir.

To ensure the accuracy and reliability of the numerical simulation, a mesh independence test was conducted. Three mesh densities were evaluated: 0.5 million, 1 million, and 1.5 million cells. Figure (6) The results were compared against the experimental data of Maranzoni et al. (2017). The errors associated with these mesh densities were 8.2%, 3.7%, and 2.56%, respectively. Based on this analysis, the 1 million-cell mesh was selected as the optimal mesh, as it provided a reasonable balance between computational cost and accuracy, with a significant reduction in error compared to the coarser mesh and only a marginal difference from the finer mesh.

The overall results of the simulations are shown in Table 3. The discharge coefficient (C_d) is obtained using the following equation.

$$C_d = \frac{3}{2} \times \frac{Q_d}{\sqrt{2g}(h-w)^{1.5}} \quad (3)$$

In this equation, W represents the crest elevation of the side weir, and h is the flow depth upstream (h_1) of the side weir (Askari and Vatankhah, 2019).

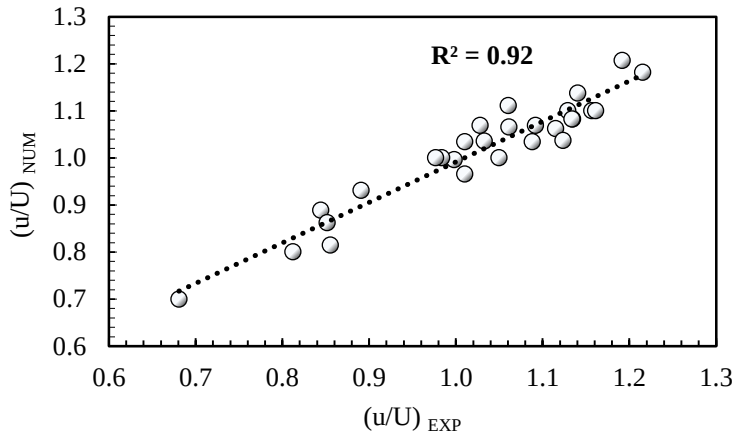

Fig. 5- Correlation of the Regression Model Based on the R^2 criterion

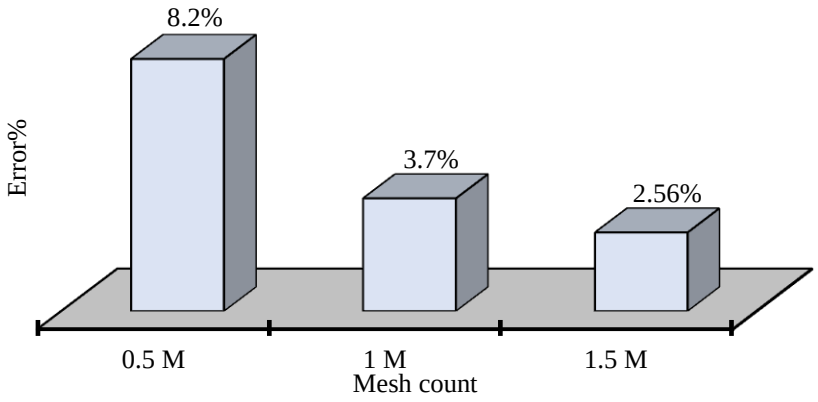

Fig. 6- Mesh independence test results

Table 3- Overall Results of the Simulations Conducted in this Study

scenarios	Q_1 (L/s)	Q_d (L/s)	Fr_1	h_1 (cm)	C_d	ε%
Control	45	28	0.359	23.12	0.902	62
T1	45	31	0.351	23.49	0.888	69
T2	45	31	0.356	23.27	0.947	69
T3	45	37	0.342	23.88	0.951	82
T4	45	28	0.360	23.25	0.913	62
T5	45	31	0.359	23.69	0.947	69
T6	45	30	0.358	23.48	0.945	67

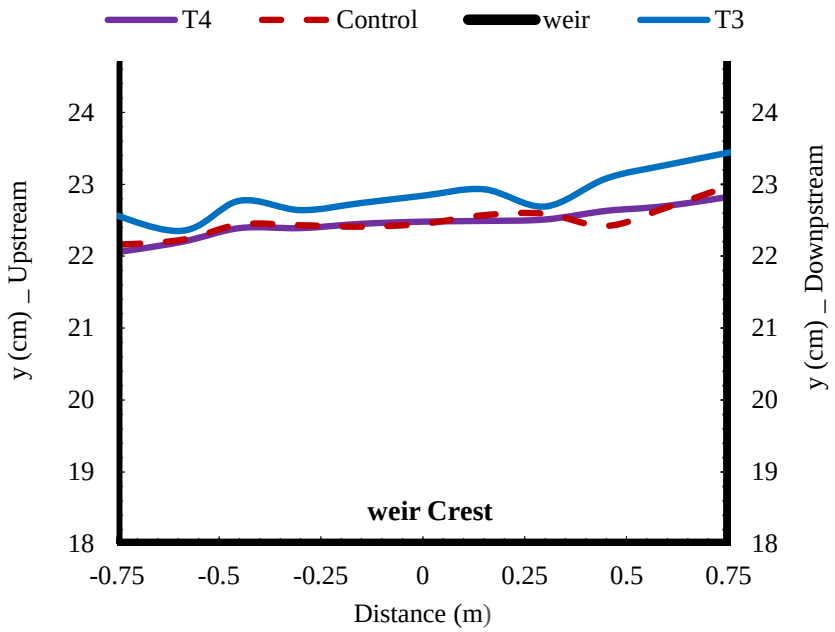

Fig. 7- Water surface profile near the crest of the converging side weir for the baseline, T3, and T4 scenarios.

Simulation T3, with an efficiency of 82%, demonstrated the best performance in directing flow towards the side weir. In this case, the side vane was installed at position X_1 with a 60-degree angle. This configuration had a significant impact compared to other positions and installation angles, resulting in a 32% increase in the diversion flow rate in this simulation compared to the baseline case. In contrast, this increase did not exceed 11% in the other simulations. At position X_2 (including simulations T4, T5, and T6), the impact of the side vane on the diversion flow rate was considerably lower than at position X_1. Notably, when the side vane was installed at a 120-degree angle, no increase in the diversion flow rate was observed. For a better understanding, Figure (7) shows the changes in water depth on the crest of the side weir for the baseline case, best performance (T3), and worst performance (T4).

The water level near the crest of the side weir noticeably increases when the side vane is installed at position X_1 with a 60-degree angle (Figure 7). This increase in water level is particularly visible in the middle and downstream areas of the weir. The findings of Bagheri and Heidarpour (2012) indicate that a significant portion of the flow is discharged from the lower downstream end of the weir. Therefore, the increased depth in the middle and downstream areas of the weir in simulation T3 has a notable effect on the diversion flow rate. In contrast, in simulation

T4 and other simulations where the side vane is installed at position X_2, the impact of the side vane on the depth profile of the water is not sufficient to increase the diversion flow rate from the side weir. This is because the range of influence of the side vane in these cases is more concentrated in areas farther from the side weir, thus having a lesser effect on directing flow towards the weir.

In Figure (8), the longitudinal velocity variations for the baseline simulation and simulation T3, which demonstrated the best performance in increasing the diversion flow rate from the side weir, are shown. It is clearly observed that with the presence of the side vane, a low-velocity region is created around the S.V. (Side Vane), while the flow velocity near the crest of the weir is maintained. This phenomenon results in a change in the flow direction and enhances the flow towards the side weir.

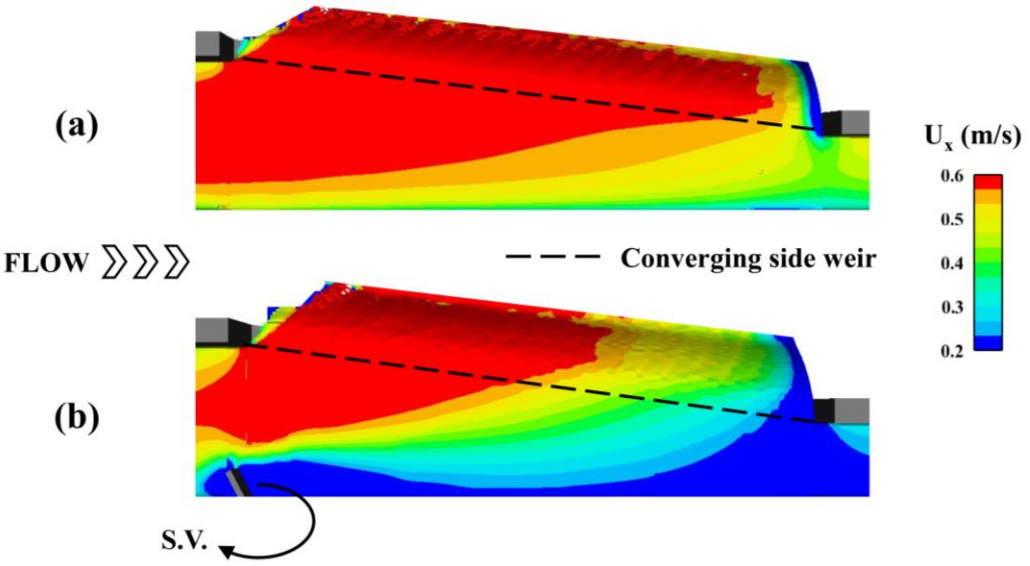

Fig. 8- Longitudinal Velocity Variations in the Converging Side Weir Area: (a) Control, (b) T3

In Figure (8) it is generally observed that with the presence of the side vane, the flow velocity in the area of the side weir has decreased. This reduction in velocity has contributed to creating conditions that allow the flow to be directed more effectively towards the side weir.

Kalateh and Aminvash (2023) conducted a study on side weirs under both subcritical and supercritical flow regimes. Their findings showed that a reduction in flow velocity could significantly increase the weir discharge. They attributed this phenomenon to the fact that, with higher velocities, the lateral flow may not have enough time to enter the side channel from the weir. In fact, as the main flow velocity increases, the time required for the lateral movement of water towards the weir decreases, which results in a reduction in the weir discharge. In Figure (9), the streamlines for simulation T3 are shown. Figure (8) raises the question that the reduction in velocity downstream might cause the flow lines to separate in the downstream area. However, the drawn streamlines clearly demonstrate that the low-velocity region after the side vane (S.V.) directs the flow towards the side weir.

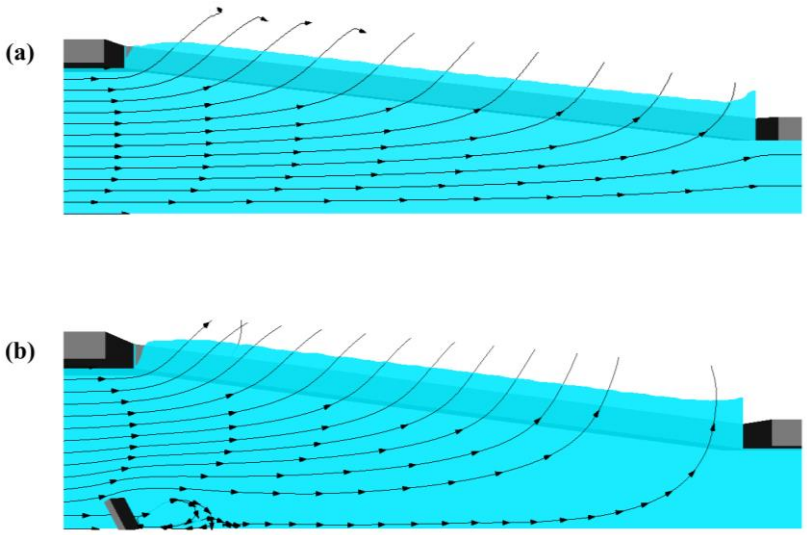

Fig. 9- Streamlines in Simulations: (a) Control, (b) T3

Contrary to the ambiguity raised by Figure (8), the streamlines in Figure 9 clearly show that separation does not occur downstream. Instead of separation, the flow is continuously directed towards the side weir.

To precisely evaluate the performance of the converging side weir in the best scenario (T3) and compare it with the baseline scenario, three baffles were installed at the upstream, middle, and downstream sections of the weir to measure the outflow discharge from each section separately. In the baseline scenario, the outflow discharges were measured as 9.5, 9.5, and 9 L/S, respectively, indicating a relatively uniform flow distribution along the weir. However, in scenario T3, where the side plate was installed at a 60-degree angle and positioned at X_1, the outflow discharges increased to 11.5, 12.1, and 13.4 L/S, respectively.

The results show that the structure had the most significant impact on the downstream section of the weir. The substantial increase in discharge at the downstream end (49%) indicates that the side structure more effectively directed the flow toward the downstream section, thereby enhancing the hydraulic efficiency in this region.

To accurately analyze the effect of the side vane on the flow hydraulics in the side weir, the depth-wise and transverse velocity distribution at the mid-section of the side weir is examined in Figure (10) for both the baseline and T3 scenarios. Since the vane is installed at the crest level of the weir, its influence on the depth-wise velocity distribution is significantly limited. However, the velocity reduction observed in Figure (8), which was identified as a key factor in increasing the diversion flow, is also evident in this distribution. Compared to the baseline scenario, where the velocity distribution is more uniform, the presence of the vane causes the velocity distribution, particularly near the water surface, to shift closer to the weir crest. Furthermore, the presence of the vane reduces the velocity near the opposite wall of the weir by 47% and concentrates the maximum velocity toward the crest.

 DOI: 10.22055/jise.2025.48446.2145

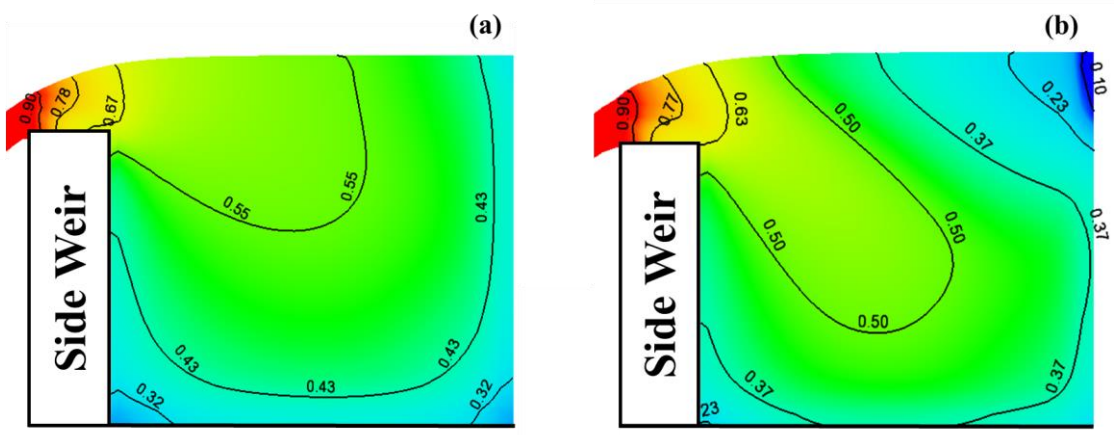

Fig. 10 Investigation of the depth-wise and transverse velocity distribution at the mid-section of the side weir: (a) Control, (b) T3

Compared to the study by Shahriari et al. (2024), where a guiding structure was installed on the crest of the side weir, resulting in a 76% efficiency (with the best performance observed when the structure was positioned at the midsection of the weir), the present study demonstrates a superior outcome. By installing the structure on the opposite wall of the side weir and at the upstream position, the efficiency increased to 82%, which is 6% higher than the result reported by Shahriari et al. (2024). This difference highlights the significant impact of the structure's installation position on improving the side weir's efficiency.

Conclusion

The use of additional elements and structures to increase the diversion flow of side weirs has always been a topic of interest in hydraulic research. Structures installed on the channel bed, even when the water level is below the weir crest, influence the hydraulics of the flow. While these structures can help increase the diversion flow of the weir, they may cause a reduction in the water level in the main channel, which could create problems for downstream structures, such as an inverted siphon.

One of the key advantages of this study is the introduction of a side vane installed at the weir crest level on the opposite wall of the weir. This vane functions similarly to an automatic structure, meaning it only diverts excess flow towards the weir when the water level rises above the normal level (the weir crest). Otherwise, it has no impact on the hydraulics of the flow in the main channel.

The results of this study showed that installing the side vane upstream of the weir with a 60-degree angle relative to the wall can increase the diversion flow of the converging side weir by 32% compared to the baseline scenario (without the side vane). This increase is mainly due to changes in the water surface profile and the formation of a low-velocity zone around the side vane. Additionally, the findings indicate that the performance of the side vane is highly dependent on its position and installation angle. Simulations revealed that in other positions and angles, the impact of the side vane on increasing diversion flow diminishes.

Acknowledgement

We are grateful to the Research Council of Shahid Chamran University of Ahvaz for financial support (GN: SCU.WH1402.31370).

References

1- Abbasi, S., Fatemi, S., Ghaderi, A. and Di Francesco, S., 2020. The effect of geometric parameters of the antivortex on a triangular labyrinth side weir. *Water*, *13*(1), p.14. Doi: https://doi.org/10.3390/w13010014.

2- Afaridegan, E., Amanian, N., Haghiabi, A., Parsaie, A., and Goodarzi-Mohammadi, A. 2023. Numerical investigation of modified semi-cylindrical weirs. *Water Resources Management*, *37*(9), pp.3715-3728. Doi: https://doi.org/10.1007/s11269-023-03523-y.

3- Askari, R. and Vatankhah, A., 2019. Theoretical and Experimental Study of Circular-Crested Trapezoidal Side Weir in Subcritical Flow Regime. *Iranian Journal of Soil and Water Research*, *50*(5), pp.1169-1181. Doi: 10.22059/ijswr.2018.262443.667972. (In Persian).

4- Azimi, H. and Shabanlou, S., 2015. The flow pattern in triangular channels along the side weir for subcritical flow regime. *Flow Measurement and Instrumentation*, *46*, pp.170-178. Doi: https://doi.org/10.1016/j.flowmeasinst.2015.04.003.

5- Bagheri Seyyed Shekari, N., Eghbalzadeh, A., Javan, M. (2018). 'The Effect of Downstream Water Depth on Hydraulic Jump Characteristics Along Side Weir', *Water and Soil Science, 28(3)*, pp. 195-208. (In Persian).

6- Bagheri, S. and Heidarpour, M., 2012. Characteristics of flow over rectangular sharp-crested side weirs. *Journal of Irrigation and Drainage engineering*, *138*(6), pp.541-547. Doi: https://doi.org/10.1061/(ASCE)IR.1943-4774.0000433.

7- Emiroglu, M.E., Kaya, N. and Agaccioglu, H., 2010. Discharge capacity of labyrinth side weir located on a straight channel. *Journal of irrigation and drainage engineering*, *136(1)*, pp.37-46. Doi: https://doi.org/10.1061/(ASCE)IR.1943-4774.0000112.

8- Ghanbari, R. and Heidarnejad, M., 2020. Experimental and numerical analysis of flow hydraulics in triangular and rectangular piano key weirs. *Water science*, *34(1)*, pp.32-38. Doi: https://doi.org/10.1080/11104929.2020.1724649.

9- Ghazizadeh, F. and Moghaddam, M.A., 2016. An experimental and numerical comparison of flow hydraulic parameters in circular crested weir using Flow3D. *Civil Engineering Journal*, *2(1*), pp.23-37. Doi: 10.28991/cej-2016-00000010.

10- Ghorbannia, D. and Eghbalzadeh, A., 2018. Numerical study of the effect of length change on the flow pattern around a side weir in a converging channel. *Acta Mechanica*, *229*, pp.4101-4111. Doi: https://doi.org/10.1007/s00707-018-2215-2.

11- Honar, T. and Javan, M., 2008. Discharge Coefficient in Oblique Side Weirs. *Iran Agricultural Research*, *25(1.2)*, pp.27-36. Doi: 10.22099/iar.2008.184

12- Kalateh, F., Aminvash, E. (2023). 'Numerical Simulation of the Effect of Channel bed Slope on the Hydraulic Performance of Sharp-Crested Rectangular Side Weir with Subcritical and Supercritical Regimes', *Iranian Journal of Soil and Water Research, 54(1)*, pp. 67-84. Doi: 10.22059/ijswr.2023.354381.669440. (In Persian).

13- Karimi, M., Attari, J., Saneie, M. and Jalili Ghazizadeh, M.R., 2018. Side weir flow characteristics: comparison of piano key, labyrinth, and linear types. *Journal of Hydraulic Engineering*, *144*(12), p.04018075. Doi: https://doi.org/10.1061/(ASCE)HY.1943-7900.0001539.

14- Kartal, V. and Emiroglu, M.E., 2022. Experimental analysis of combined side weir-gate located on a straight channel. *Flow Measurement and Instrumentation*, *88*, p.102250. Doi: https://doi.org/10.1016/j.flowmeasinst.2022.102250.

15- Khassaf, S.I., Attiyah, A.N. and Al-Yousify, H.A., 2016. Experimental investigation of compound side weir with modeling using computational fluid dynamic. *International Journal of Energy and Environment*, *7*(2), p.169.

16- Maranzoni, A., Pilotti, M. and Tomirotti, M., 2017. Experimental and numerical analysis of side weir flows in a converging channel. *Journal of Hydraulic Engineering*, *143*(7), p.04017009. Doi: https://doi.org/10.1061/(ASCE)HY.1943-7900.0001296.

17- Mirzaei, K. and Sheibani, H.R., 2021. Experimental investigation of arched sharp-crested weir flow and comparing it with rectangular weir. *Iranian Journal of Science and Technology, Transactions of Civil Engineering*, *45*(2), pp.1039-1048. Doi: https://doi.org/10.1007/s40996-020-00425-6.

18- Mohamadalipourahari, A., Bakhtiari Arkasi, A. and Jalilighazizadeh, M. 2021. Numerical study of the flow velocity distribution over rectangular side weirs. *Modares Civil Engineering journal, 21*, pp.113-126 (In Persian).

19- Noroozi, B., Bazargan, J. and Safarzadeh, A., 2021. Introducing the T-shaped weir: a new nonlinear weir. *Water Supply*, *21*(7), pp.3772-3789. Doi: https://doi.org/10.2166/ws.2021.144.

20- Parsaie, A., Moradinejad, A., and Haghiabi, A. H. 2018. Numerical modeling of flow pattern in spillway approach channel. *Jordan Journal of Civil Engineering*, *12*(1).

21- Parsaie, A., Shareef, S. J. S., Haghiabi, A. H., Irzooki, R. H., and Khalaf, R. M. 2022. Numerical simulation of flow on circular crested stepped spillway. *Applied Water Science*, *12*(9), p.215. Doi: https://doi.org/10.1007/s13201-022-01737-w.

22- Parsi, E., Allahdadi, K., Bahrebar, A. and Farhadi, R. 2021. Effect of downstream contraction on side weirs discharge. *Iranian Journal of Irrigation & Drainage, 15(2),* pp.455-466. Doi: 20.1001.1.20087942.1400.15.2.18.0. (In Persian).

23- Saffar, S., Safaei, A., Aghaee Daneshvar, F. and Solimani Babarsad, M., 2023. Flow-3D numerical modeling of converged side Weir. *Iranian Journal of Science and Technology, Transactions of Civil Engineering*, *48*(1), pp.431-440. Doi: https://doi.org/10.1007/s40996-023-01077-y.

24- Shahriari, A., Daryaee, M., Kashefipour, S., and Zayeri, M. 2024. Numerical Simulation of the Effect of Single Guide Vane Installation on the Hydraulic Performance of Side Weirs in Converging Channels. *Iranian Journal of Science and Technology, Transactions of Civil Engineering*,. Doi: https://doi.org/10.1007/s40996-024-01707-z.

25- Taghavi, M. and Ghodousi, H., 2016. A comparison on discharge coefficients of side and normal weirs with suspended flow load using Flow3D. *Indian J. Sci. Technol*, *9*, pp.1-11. Doi: 10.17485/ijst/2016/v9i3/78537.

26- Vatankhah, A.R., 2013. Water surface profile along a side weir in a parabolic channel. *Flow Measurement and Instrumentation*, *32*, pp.90-95. Doi: https://doi.org/10.1016/j.flowmeasinst.2013.04.010.

27- Zarei, S., Yosefvand, F. and Shabanlou, S., 2020. Discharge coefficient of side weirs on converging channels using extreme learning machine modeling method. *Measurement*, *152*, p.107321. Doi: https://doi.org/10.1016/j.measurement.2019.107321.

© 2025 Shahid Chamran Universiry of Ahvaz, Ahvaz, Iran. This article is an open access article distributed under the terms and conditions of the Creative Commons Attribution 4.0 International (CC BY 4.0 license) (http://creativecommons.org/licenses/by/4.0/).